Tropical High Cloud Feedback Relationships to Climate Sensitivity

EMMA DAWSON[a] AND KATHLEEN A. SCHIRO[a]

[a] *University of Virginia, Charlottesville, Virginia*

(Manuscript received 16 April 2024, in final form 31 August 2024, accepted 28 October 2024)

ABSTRACT: Clouds constitute a large portion of uncertainty in predictions of equilibrium climate sensitivity (ECS). While low cloud feedbacks have been the focus of intermodel studies due to their high variability among global climate models, tropical high cloud feedbacks also exhibit considerable uncertainty. Here, we apply the cloud radiative kernel technique of Zelinka et al. to 22 models across the CMIP5 and CMIP6 ensembles to survey tropical high cloud feedbacks and analyze their relationship to ECS. We find that the net high cloud feedback and its altitude and optical depth feedback components are significantly positively correlated with ECS in the tropical mean. On the other hand, the tropical mean high cloud amount feedback is not correlated with ECS. These relationships are most pronounced outside of areas of strong climatological ascent, suggesting the importance of thin cirrus feedbacks. Finally, we explore connections between high cloud feedbacks, climate sensitivity, and mean state high cloud properties. In general, high ECS models are cloudier in the upper troposphere but have a thinner high cloud population. Moreover, we find that having more thin cirrus in the mean state relates to more positive high cloud altitude and optical depth feedbacks, and it either amplifies or dampens the high cloud amount feedback depending on the large-scale dynamical regime (amplifying in descent and dampening in ascent). In summary, our analysis highlights the importance of tropical high cloud feedbacks for driving intermodel spread in ECS and suggests that mean state high cloud characteristics might provide a unique opportunity for observationally constraining high cloud feedbacks.

SIGNIFICANCE STATEMENT: Clouds play an important role in modulating the effects of climate change through feedback processes involving changes to their amount, altitude, and opacity. In this study, we seek to understand how changes to tropical high clouds under warming are related to the magnitude of warming that global climate models simulate. We find that tropical high cloud feedbacks robustly relate to the amount of warming a model predicts and that warmer models tend to have a thinner tropical high cloud climatology. Our results highlight a potential opportunity to form a new constraint using these relationships in order to narrow the spread of warming estimates among global climate models.

KEYWORDS: Atmosphere; Tropics; Climate sensitivity; Cloud radiative effects; Feedback; Model comparison

1. Introduction

Cloud feedbacks represent the largest contributor to overall uncertainty in climate sensitivity and the transient climate response to greenhouse gas forcing (Soden and Held 2006; Dufresne and Bony 2008; Vial et al. 2013; Caldwell et al. 2016), increasing in spread from phase 5 of the Coupled Model Intercomparison Project (CMIP) to CMIP6 (Zelinka et al. 2020). The net cloud feedback is calculated as the summation of longwave and shortwave cloud radiative effects that result from changes to clouds with warming. Thus, decomposition techniques are often employed to isolate the physical processes underlying these changes and distinguish between feedback components that have a consistent sign and magnitude across models and components that exhibit intermodel spread. Commonly, cloud feedbacks are divided into the cloud amount, altitude, and optical depth feedbacks. These cloud feedback components describe the radiative effect of changes to total cloud amount, redistribution of cloud fraction across altitudes, and redistribution across optical thicknesses with warming, assuming the other components are held constant (Zelinka et al. 2012b). In addition to decomposition by physical process, cloud feedbacks are often separated by their prevalence at different altitudes. For example, the low cloud amount feedback has garnered significant attention because its magnitude and sign vary among global climate models (GCMs) and it contributes the most variance to the global cloud feedback (Bony and Dufresne 2005; Caldwell et al. 2016; Zelinka et al. 2016) despite the general consensus that its value is positive (Ceppi et al. 2017; Sherwood et al. 2020).

Although low cloud feedbacks are highly variable, high cloud feedbacks also exhibit substantial intermodel spread. For example, using cloud radiative kernels, Zelinka et al. (2022) found that the high cloud altitude feedback has the largest number of models that fall outside of the expert-assessed ranges published by Sherwood et al. (2020), which serve as a best estimate of feedback values by combining historical data, the paleoclimate record, and current process understanding in a Bayesian framework. Tropical high clouds have risen in observations over the last two decades (Richardson et al. 2022; Raghuraman et al. 2024) and have been shown to increase in altitude in response to

Supplemental information related to this paper is available at the Journals Online website: https://doi.org/10.1175/JCLI-D-24-0218.s1.

Corresponding author: Emma Dawson, emd6wn@virginia.edu

DOI: 10.1175/JCLI-D-24-0218.1

interannual surface warming (Zhou et al. 2014; Zelinka and Hartmann 2011). The decrease in cloud-top pressure (CTP) with warming is grounded in physical theory first explained by Hartmann and Larson (2002). They put forth the fixed anvil temperature (FAT) hypothesis, which argues that convective detrainment preferentially occurs at a fixed temperature that coincides with the temperature at which the efficacy of clear-sky radiative cooling by water vapor declines. This implies that cloud tops should remain at the same temperature under climate change, maintaining a constant longwave emission to space despite rising surface temperatures, which results in a positive feedback. This argument was later modified by Zelinka and Hartmann (2010), who proposed the proportionally higher anvil temperature (PHAT) hypothesis. They argue that an increase in upper-tropospheric static stability under warming results in a slight warming of cloud tops as they rise but less than the magnitude of the surface. The combination of observational evidence and support from theory has led to a consensus that the high cloud altitude feedback is robustly positive (Zelinka et al. 2016; Ceppi et al. 2017), and CMIP6 models accurately reflect this (Zelinka et al. 2022). However, the magnitude of the altitude feedback varies significantly among models despite a solid comprehension of its underlying mechanisms, suggesting that further work is needed to understand the source of its intermodel variability.

In addition to the high cloud altitude feedback, Zelinka et al. (2022) conclude that tropical anvil cloud feedbacks remain uncertain, finding that 8 out of 19 GCMs produce values above the expert-assessed value noted in Sherwood et al. (2020). Reduction in anvil cloud fraction under warming has been supported by thermodynamic arguments first referred to as an "Iris Feedback" by Lindzen et al. (2001). They postulate that high clouds in the tropics contract with surface warming due to enhanced precipitation efficiency, which acts as an adaptive mechanism to allow for enhanced longwave cooling. Later, Zelinka and Hartmann (2010) and Bony et al. (2016) formed the "Stability Iris" hypothesis, which argues that increased upper-tropospheric static stability reduces convective outflow, resulting in a reduction in high cloud fraction at the altitude of peak high cloud coverage. While observations indicate that high clouds reduce with warming (Saint-Lu et al. 2020; Su et al. 2017; Liu et al. 2017), idealized modeling studies show mixed results (Cronin and Wing 2017; Wing et al. 2020; Ohno et al. 2019), and several recent studies infer a near-neutral high cloud amount feedback (McKim et al. 2024; Chao et al. 2024). Furthermore, factors such as model resolution (Jeevanjee and Zhou 2022), sensitivity of cloud lifetime to warming (Seeley et al. 2019; Beydoun et al. 2021), and intermodel variability in changes to ascent area (Su et al. 2017; Schiro et al. 2019) contribute to the intermodel spread of the response of tropical anvil cloud extent to warming across models, complicating the analysis of the iris feedback among GCMs. Additionally, because the radiative effect of tropical high clouds varies significantly across clouds of different optical thicknesses, changes in the relative abundance of tropical high clouds across different opacities under warming can also contribute to the anvil feedback. While there is observational evidence that cirrus fraction reduces with interannual warming in the tropical western Pacific (Choi et al. 2017), the sign of the anvil optical depth feedback remains inconclusive (Gasparini et al. 2021; Sokol et al. 2024; Zelinka et al. 2022), with limited analysis of the optical depth feedback across GCMs (as also pointed out by Ceppi et al. 2017) and a lack of theoretical support unlike the high cloud altitude and amount feedbacks. Thus, despite improved understanding of models' representation of the climate system and the development of physical theories, persistent uncertainty exists around tropical high cloud feedbacks in GCMs.

Analyzing relationships between the intermodel spread in climate sensitivity and present-day climate variability, or variability in mean state characteristics across models, can be a powerful tool to constrain the spread of equilibrium climate sensitivity, the long-term global mean change in surface temperature following a doubling of CO_2, through an emergent constraint framework (Klein and Hall 2015). Several mean parameters related to tropical clouds have been highlighted for their relationship to climate sensitivity, including relative cloud fraction between the tropics and midlatitudes (Volodin 2008) and tropical cloud albedo (Siler et al. 2018). Characteristics of tropical boundary layer clouds have been a particular area of interest for establishing connections between mean state parameters and ECS (Zhai et al. 2015; Brient et al. 2016; Brient and Schneider 2016). However, Po-Chedley et al. (2019) highlight a relationship between changes in tropical upper-tropospheric cloud fraction and model climatology, successfully predicting the rise of high clouds in the tropics from the mean state cloud field assuming that clouds track with isotherms and that warming in the tropics follows a dilute moist adiabat. This finding suggests that mean state tropical high cloud fraction relates to the behavior of high clouds under warming, which produce cloud feedbacks. Thus, further analysis of how climatological high cloud fields in the tropics relate to high cloud feedbacks and the resulting intermodel spread in climate sensitivity presents an opportunity to expand on the existing emergent constraint literature.

This paper aims to explore whether a relationship exists between the intermodel spread in tropical high cloud feedbacks and the intermodel spread in climate sensitivity. We use the cloud radiative kernel technique of Zelinka et al. (2012a, 2013) to visualize cloud feedback components across different cloud types and isolate differences between relatively high and low ECS models across our ensemble. We conclude by examining differences in mean state high cloud characteristics across models as they may relate to the intermodel spread in high cloud feedbacks.

2. Methods

We analyze output from 22 models from the CMIP5 (8 models) and CMIP6 (14 models) model ensembles. Models were chosen based on availability of variables necessary for the application of the cloud radiative kernels of Zelinka et al. (2012a). We chose 22 models that provided necessary output for years 1–10 and 131–140 of the abrupt-4xCO_2 runs. To remove the effects of cloud rapid adjustments from our feedback calculation and isolate temperature-mediated changes to clouds, we choose to compute feedbacks relative to years 1–10 of the abrupt-4xCO_2 experiment. Hereafter, years 1–10 of the abrupt-4xCO_2 experiment will be referred to as the "control" run and years 131–140 will be referred to as the "perturbed" run. To characterize mean state high cloud fraction, we utilize output from piControl for 17 models and piClim-Control for five additional models as was done in Zelinka et al. (2022), averaging from years 121 to 130 for piControl runs or from the closest available 10-yr period and years 21–30 for the piClim-control runs.

The radiative kernel computations utilize the cloud fraction variable *clisccp* produced by the International Satellite Cloud Climatology Project (ISCCP) simulator run inline with model experiments (Klein and Jakob 1999). The ISCCP simulator applies a cloud detection algorithm that considers only radiatively relevant cloud coverage in terms of top-of-atmosphere fluxes, eliminating issues of intermodel differences in cloud overlap assumptions (Zelinka et al. 2012a). The *clisccp* variable yields a cloud fraction matrix representing 49 cloud types in CTP–optical depth τ space across seven discretized CTP categories and seven τ groups. The use of this metric of cloud fraction allows for decomposition of mean state cloud fraction and radiative feedbacks into specific cloud types rather than reporting a bulk quantity.

Normalized cloud fraction anomaly matrices were produced by subtracting the control run *clisccp* matrix from the perturbed run *clisccp* matrix and normalizing by the global average change in surface temperature dT_s following interpolation to a common $2° \times 2.5°$ grid. We computed longwave and shortwave feedbacks by multiplying the normalized cloud fraction anomaly histograms by the cloud radiative kernels from Zelinka et al. (2012a), mapping the kernels to the corresponding latitude and surface albedo at each grid point. The net cloud feedback was calculated as the sum of the longwave and shortwave cloud feedback histograms. Each bin of the radiative kernels represents the radiative effect in W m^{-2} resulting from a percent increase in cloud fraction of that cloud type. As a result, this computation produces the radiative impact of a change in a particular cloud type between the control and perturbed scenarios.

We further decompose the total cloud feedback into cloud amount, altitude, and optical depth feedbacks using the methods of Zelinka et al. (2013). The cloud feedback decomposition was performed by dividing the cloud fraction anomaly histograms into two components and the radiative kernel into four components, yielding a four-term decomposition of the net cloud feedback into the cloud amount, altitude, and optical depth feedbacks in addition to a residual term. We perform this computation separately for the clouds higher than 680 hPa and lower than 680 hPa, represented by the five rows of lowest pressure and the two rows of highest pressure of the cloud fraction matrix as was done by Zelinka et al. (2016). This division separates free tropospheric from boundary layer clouds, allowing for their feedbacks to be computed separately and devoid of unrealistic influence from the other cloud grouping. Due to the anomalous assignment of partly cloudy pixels to low optical depth bins by the ISCCP product (Pincus et al. 2012), we choose to consider only clouds of optical depths $0.3 < \tau < 380$.

We analyze the net high cloud feedback, high cloud altitude feedback, high cloud optical depth feedback, and the high cloud amount feedback. We consider tropical mean correlations between each cloud feedback component and ECS in addition to the spatial distribution of the correlation between values of the cloud feedbacks at each grid box and ECS. The net feedback, which in part determines the magnitude of climate sensitivity, is traditionally decomposed into Planck, water vapor, lapse rate, albedo, and cloud feedback terms (Caldwell et al. 2016). Thus, while all cloud feedback components contribute to the net feedback as summed parts, cloud feedback components may be correlated or anticorrelated with ECS. Due to the causal relationship between the cloud feedback magnitude and ECS, we interpret a positive correlation between a cloud feedback component and ECS as indication that the intermodel spread in the cloud feedback is driving intermodel variability in ECS; an anticorrelation between a cloud feedback component and ECS suggests that, while serving as a portion of net feedback, the variability in the cloud feedback component among models is not strongly influencing the intermodel spread in ECS. This isolates particular cloud feedback components and regions as the most important for determining the magnitude of ECS and highlights opportunities for constraint.

To analyze the differences in cloud feedbacks and mean state cloud fraction between high and low ECS models, the ensemble was divided into high and low ECS groups and averages were taken across the highest seven and lowest seven models falling into these categories, respectively, corresponding to ECS values of ≥4.7 and ≤3.7 K. ECS values were taken from Zelinka et al. (2020) or calculated using the standard Gregory method (Gregory et al. 2004) when not available. We analyze mean state cloud fraction across thick, thin, and total high cloud fraction. Here, we define high cloud fraction and high cloud feedbacks as the lowest five pressure bins of the ISCCP matrix, representing the region from 680 to 50 hPa. Feedbacks are scaled by their fractional coverage of Earth's surface. Thick high cloud fraction is treated as the sum of high clouds in the highest three optical depth bins ($9.4 < \tau < 380$), thin high cloud fraction is defined as high clouds in the lowest three optical depth bins ($0.3 < \tau < 9.4$), and total high cloud fraction is the sum across all six optical depth categories ($0.3 < \tau < 380$). Finally, when considering feedbacks and mean state cloud characteristics across different dynamical regimes, we consider tropical ascent regions to be where vertical pressure velocity at 500 hPa (ω_{500}) is less than 0 hPa day^{-1} and descent regions as $\omega_{500} > 0$ hPa day^{-1}.

3. Results

a. High cloud feedbacks

To analyze the relationship between the tropical net high cloud feedback and climate sensitivity, we correlate the net high cloud feedback with ECS at each grid box across the tropics (Fig. 1a) and tropics-wide (Fig. 1b), yielding strongly positive, statistically significant relationships throughout much of the tropics, especially outside of areas of strongest ascent.

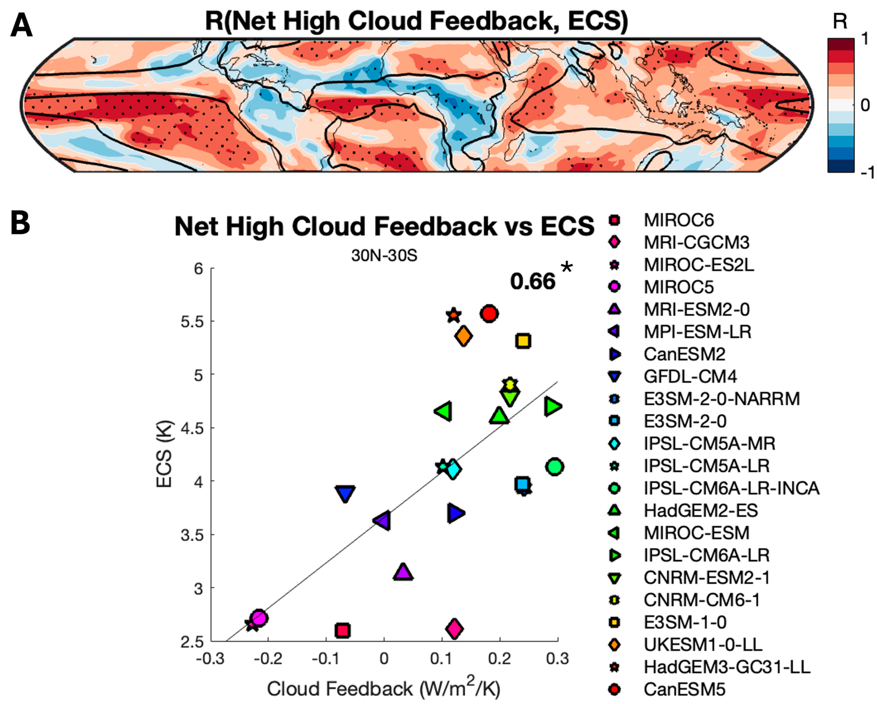

FIG. 1. (a) Spatial correlation of the local net high cloud feedback and ECS. The multimodel mean control experiment $\omega_{500} = 0$ hPa day^{-1} contour is depicted by the thick black line. Significance at $\alpha = 0.05$ is indicated by stippling. (b) Tropical mean relationship between the net high cloud feedback and ECS. The Pearson correlation coefficient is in bold, and statistical significance at $\alpha = 0.05$ is indicated by an asterisk. Models are listed in order of increasing ECS.

The strongest positive correlations exist in areas of climatological descent, such as in the eastern equatorial Pacific. Correlating the net high cloud feedback constrained to each model's control run descent region and ECS yields a coefficient of $R = 0.71$ (Fig. S1b in the online supplemental material). Within areas of deep convection, where climatological abundance of high clouds is greatest, the net high cloud feedback is more weakly correlated or anticorrelated with ECS (Fig. 1a), albeit the tropics-wide ascent region correlation is $R = 0.53$ (Fig. S1a). These results suggest that high cloud feedbacks on convective margins and in areas of climatological descent are more strongly related to the magnitude of simulated warming within a model than high cloud feedbacks in the deep tropics.

Next, we decompose the tropical mean net high cloud feedback into its amount, altitude, and optical depth components and correlate these feedbacks with ECS (Fig. 2). The total high cloud altitude feedback is positively correlated with ECS ($R = 0.55$; Fig. 2a). The high cloud altitude feedback is expected to be robustly positive based on physical arguments posited by the FAT hypothesis (Hartmann and Larson 2002) and the PHAT hypothesis (Zelinka and Hartmann 2010) in addition to observations (Zelinka and Hartmann 2011; Xu et al. 2007) and evidence from GCMs that show an increase in high cloud altitude under warming (Bony et al. 2016; Zelinka and Hartmann 2010). Zelinka et al. (2022) confirm this in GCMs, finding that the global mean high cloud altitude feedback is either positive or near zero across an ensemble of 19 models. In line with these results, we find that the tropical mean high cloud altitude feedback is positive in 20 models and near zero in the remaining two models. Of greatest significance to our analysis is the significant positive correlation shown here, which suggests that the spread of the tropical high cloud altitude feedback is a nontrivial driver of the intermodel variability in climate sensitivity.

The high cloud optical depth feedback is also positively correlated with ECS ($R = 0.54$; Fig. 2b), with 10 out of 22 models exhibiting a positive high cloud optical depth feedback corresponding to a net thinning of high clouds with warming. Increases in upper-tropospheric stability (Bony et al. 2016; Zelinka and Hartmann 2010) and a reduction in convective mass flux (Hartmann 2016) in GCMs under warming have been linked to a loss of anvil coverage. However, these arguments do not address the potential changes in the distribution of high clouds across different optical depths as they reduce in spatial extent. The disagreement in the ensemble on the sign of the high cloud optical depth feedback aligns with the uncertainty of the net radiative impact of changing high cloud opacity in GCMs that has been noted only in recent studies of intermodel variability of the optical depth feedback (Zelinka et al. 2022; Sokol et al. 2024).

The high cloud amount feedback is uncorrelated with ECS in the tropical mean ($R = 0.14$; Fig. 2c). This weak relationship suggests that variability in the tropical high cloud amount

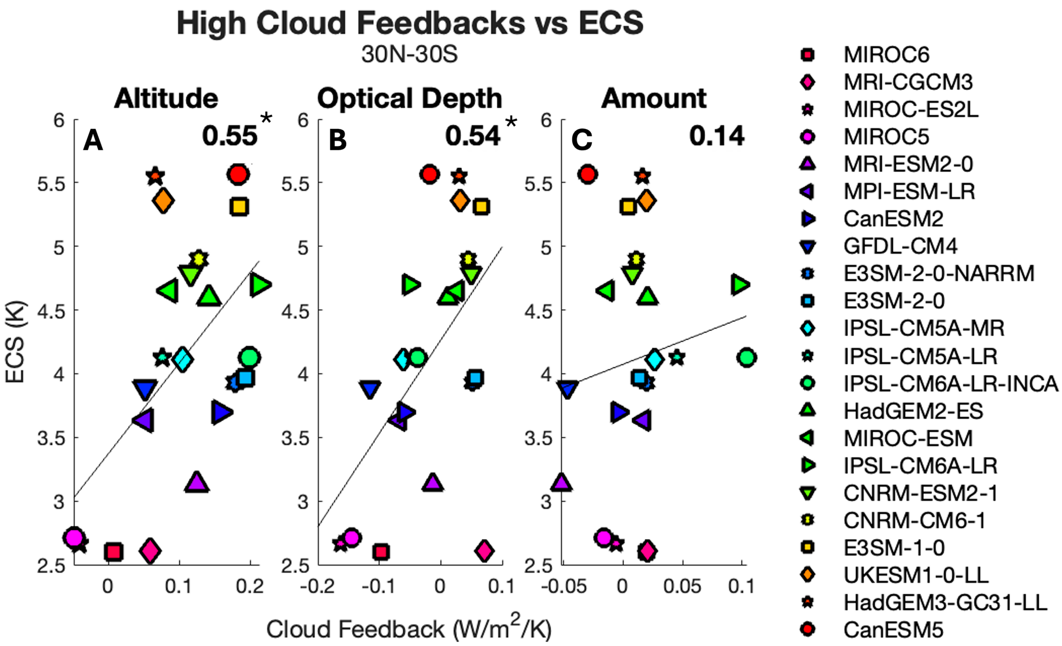

FIG. 2. As in Fig. 1b, but for tropical mean relationships between the (a) net high cloud altitude feedback, (b) net high cloud optical depth feedback, and (c) net high cloud amount feedback and ECS. The Pearson correlation coefficient is in bold, and statistical significance at $\alpha = 0.05$ is indicated by an asterisk.

feedback is not a primary driver of intermodel spread in climate sensitivity. We find that 15 models have a positive amount feedback, of which 11 show a net loss of tropical high clouds with warming (not shown). Additionally, we note that the range of the amount feedbacks across models is smaller than the range of values produced by the high cloud altitude and optical depth feedbacks, with many models clustering around 0 W m^{-2} K^{-1}. This is not surprising given that anvils have an approximately neutral radiative effect resulting from the cancellation between the large positive longwave and negative shortwave radiative effects of thin and thick clouds (Hartmann and Berry 2017). Moreover, recent observational results show a near-zero radiative effect from the contraction of high clouds (Raghuraman et al. 2024; McKim et al. 2024).

In summary, we find that the tropical mean net high cloud feedback is strongly correlated with climate sensitivity, arising from significant tropical mean correlations between the high cloud altitude feedback and high cloud optical depth feedback and ECS. Additionally, the net high cloud feedback relationship to ECS is strongest outside of the deep tropics. Next, we consider the correlation between the high cloud altitude, optical depth, and amount feedbacks with ECS in space to identify regions contributing to the tropical mean relationships of each feedback component.

1) High cloud altitude feedback

We correlate the high cloud altitude feedback at each grid box with ECS (Fig. 3a) to identify the areas that drive the tropical mean relationship (Fig. 2a). The spatial pattern of the correlation of the high cloud altitude feedback to ECS mimics the correlation pattern of the net high cloud feedback with ECS (Fig. 1a), albeit with some variations. Similar to the net high cloud feedback, the high cloud altitude feedback is correlated with ECS on convective margins and in areas of climatological descent and anticorrelated or uncorrelated with ECS across the areas of strongest ascent, particularly equatorial land regions. The exception to this pattern is the Maritime Continent and warm pool region, where the high cloud altitude feedback exhibits broad, modest correlations with ECS extending to the central and eastern Pacific. The high cloud altitude feedback composited for the seven highest ECS models (Fig. 3b) demonstrates positive high cloud altitude feedbacks across most of the tropics with the largest magnitude in the Pacific ITCZ, Congo, and West Africa regions. In contrast, the high cloud altitude feedback composited for the seven lowest ECS models (Fig. 3c) shows strong, positive high cloud altitude feedbacks that are limited to the deep convective regions of the ITCZ, Congo, and West Africa. Additionally, the low ECS composite yields modest negative high cloud altitude feedbacks in Pacific descent regions. We subtract the low ECS composite from the high composite to assess where the high cloud altitude feedback differs the most between the two groups (Fig. S2b). The central and eastern Pacific display the greatest relative difference in the high cloud altitude feedback between the composites (red shading), as is also shown for the net high cloud feedback (Fig. S2a), confirming that the local correlations in these areas previously highlighted are the main contributors to the tropical mean relationship to ECS. Further reflecting this spatial pattern, the descent region correlation between the high cloud altitude feedback and ECS is stronger ($R = 0.63$; Fig. S1d) than the ascent region correlation ($R = 0.50$; Fig. S1c), though both are statistically significant.

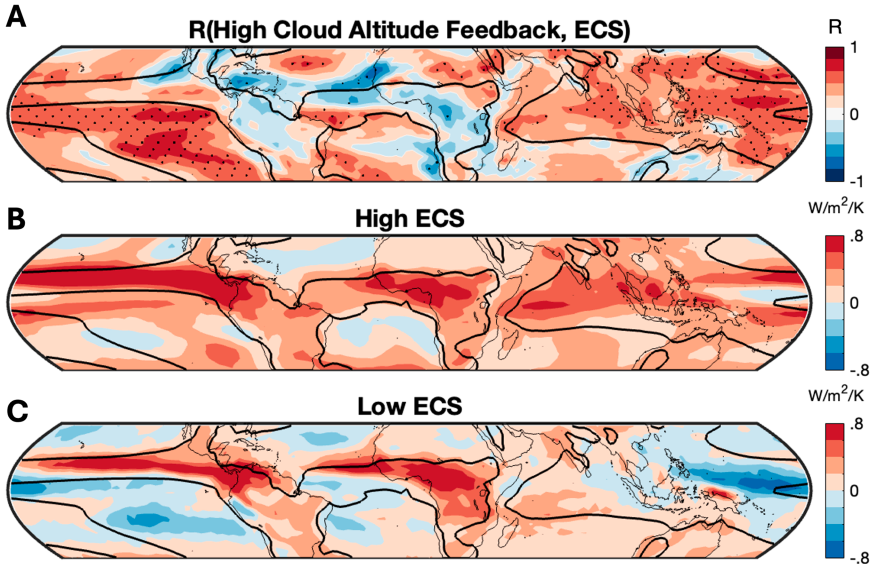

FIG. 3. (a) As in Fig. 1a, but for the spatial correlation of the local net high cloud altitude feedback and ECS. The multimodel mean control experiment $\omega_{500} = 0$ hPa day^{-1} contour is depicted by the thick black line. Significance at $\alpha = 0.05$ is indicated by stippling. (b),(c) High cloud altitude feedback for the (b) high ECS (≥4.7 K) group and (c) low ECS (≤3.7 K) group.

Maps of the high cloud altitude feedback for all 22 models, in order of increasing ECS, are displayed in Fig. S3.

2) High cloud optical depth feedback

Similar to the net high cloud feedback, the high cloud optical depth feedback is correlated with ECS on convective margins and in areas of climatological descent and anticorrelated or uncorrelated with ECS across the areas of strongest ascent (Fig. 4a). Local correlations of the optical depth feedback to ECS are weaker than the net high cloud feedback correlations to ECS, but they have a similar spatial arrangement. This pattern suggests that variability in changes to the opacity of clouds in the deep tropics under warming is a weaker driver of the spread in climate sensitivity than changes to high cloud thickness outside of ascent regions. While the deepest convective cores are found in observations primarily across tropical South America, Africa, and the Maritime Continent (Houze et al. 2015), thinner high clouds are spread more ubiquitously across the tropics (Sassen et al. 2009), which is reflected by the multimodel

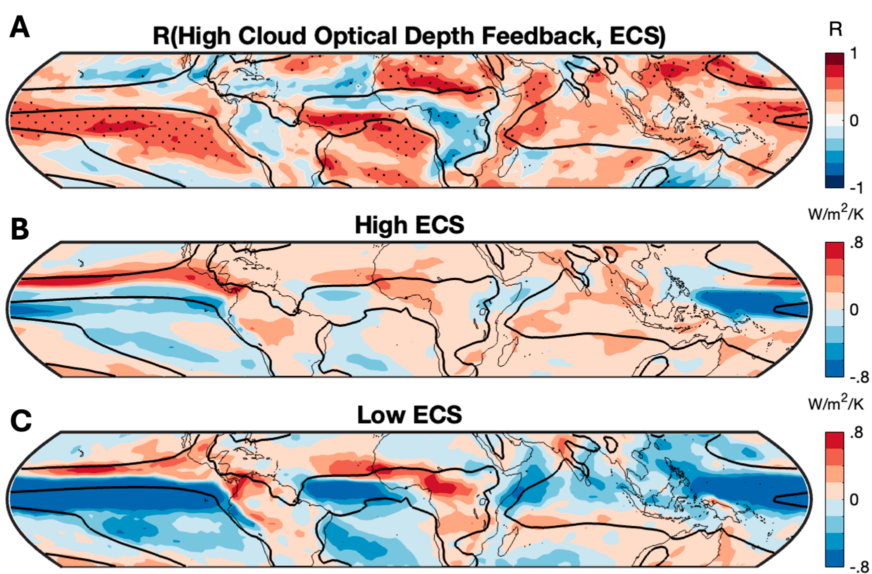

FIG. 4. As in Fig. 3, but for the high cloud optical depth feedback.

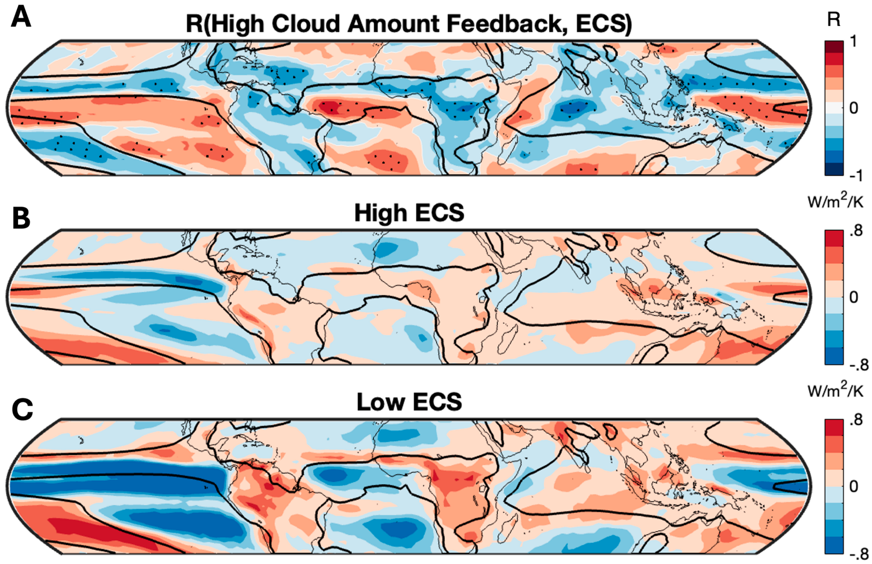

FIG. 5. As in Fig. 3, but for the high cloud amount feedback.

mean climatological distribution of high cloud opacity of our ensemble (Fig. S4). Thus, we hypothesize that changes to anvils extending away from areas of deep convection or isolated thin cirrus are primarily responsible for the overall correlation between the tropical high cloud optical depth feedback and climate sensitivity. This inference aligns with the conclusions of Sokol et al. (2024), who argue that the uncertainty in the net radiative effect of changes to anvils under warming comes primarily from changes to thin high cloud opacity in cloud-resolving models. Comparing the high and low ECS composite maps (Figs. 4b,c) shows that both sets of models experience a net thinning of high clouds along the Pacific ITCZ and equatorial Africa and South America (red shading). High ECS models experience a weaker and less extensive thickening of high clouds (blue shading) along the equatorial Pacific and Atlantic than low ECS models, which produces the greatest relative difference in the optical depth feedback between the composited groups (Fig. S2c). As with the high cloud altitude feedback, this yields a stronger correlation between the descent region high cloud optical depth feedback and ECS ($R = 0.64$; Fig. S1f) than the ascent region high cloud optical depth feedback and ECS ($R = 0.44$; Fig. S1e). Additionally, we note that the spatial pattern of the high cloud altitude feedback composite maps qualitatively matches the pattern of the high cloud optical depth feedback composite maps, which is reflected by significant positive correlations between the two feedbacks across the tropics (Fig. S5). This aligns with the findings of Zelinka et al. (2022), who suggest that a common mechanism may be driving the covariability of the cloud altitude and optical depth feedbacks. Maps of the high cloud optical depth feedback for all 22 models are shown in Fig. S6.

3) High cloud amount feedback

Finally, we consider the spatial arrangement of the correlation between the local high cloud amount feedback and ECS (Fig. 5a). The spatial pattern of the correlations between the high cloud amount feedback and ECS qualitatively mimics the patterns previously shown for the relationships of the net high cloud feedback, high cloud optical depth feedback, and high cloud altitude feedback with ECS. Generally, ascent regions are dominated by anticorrelations while convective margins or descent regions display correlations, though the strength of the relationships is weak, and the ascent region correlations are more negative here for the amount feedback than the other feedbacks. We gather that the opposing signs in ascent and descent regions contribute to the tropical mean high cloud amount feedback being weakly correlated with ECS (Fig. 2c).

Comparing the high and low ECS composite maps (Figs. 5b,c) shows that both groups of models generally see a positive high cloud amount feedback in ascent regions, corresponding to a net loss of high clouds in the deep tropics with warming (Fig. S7). Given that deep convective clouds have a high albedo, resulting in a negative cloud radiative effect, the anticorrelations in ascent regions suggest that high ECS models tend to see a lesser decrease in high cloud amount under warming in deep convective zones than low ECS models. Additionally, both groups of models see a negative high cloud amount feedback across descent regions; correlations in these areas can be interpreted as a greater increase in high cloud amount with warming for low ECS models than high ECS models (Fig. S7). We caveat these conclusions by noting that neither the ascent region correlation ($R = -0.24$; Fig. S1g) nor the descent region correlation ($R = 0.44$; Fig. S1h) is particularly strong. Maps of the high cloud amount feedback for all 22 models are shown in Fig. S8.

In summary, our analysis suggests that variability in tropical high cloud feedbacks is significantly related to the spread in climate sensitivity, especially outside of regions of strongest climatological ascent. The high cloud altitude and optical

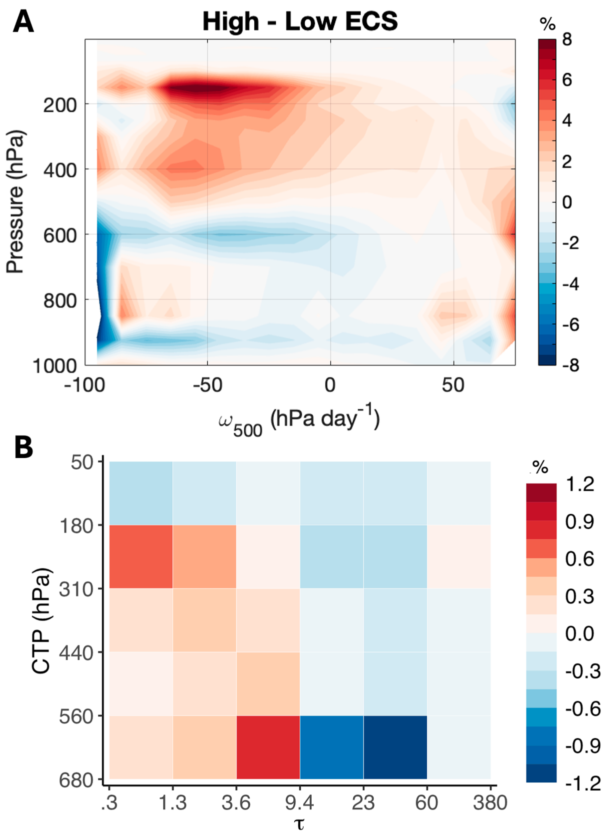

FIG. 6. (a) Difference of composited piControl/piClim-control experiment tropical mean (30°N–30°S) cloud fraction conditionally averaged on pressure and ω_{500} between the high ECS (≥4.7 K) and low ECS (≤3.7 K) groups from the *cl* output. (b) Difference in piControl/piClim-control experiment cloud fraction histograms between the high ECS and the low ECS groups from the *clisccp* output. Only the free tropospheric (680–50 hPa) portion of the histogram is shown.

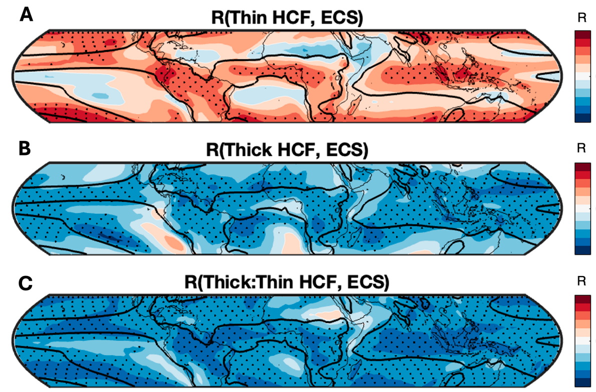

FIG. 7. As in Fig. 1a, but for (a) mean state thin HCF and ECS, (b) mean state thick HCF and ECS, and (c) mean state ratio of thick to thin HCF and ECS.

depth feedbacks contribute most strongly to this relationship. Next, we analyze how mean tropical high cloud characteristics vary with climate sensitivity and tropical high cloud feedbacks to evaluate the potential for mean state cloud fraction to observationally constrain the feedbacks.

b. *Mean state relationships*

Su et al. (2014) suggest that high ECS models have higher mean state high cloud fraction than low ECS models. Since we found robust correlations between high cloud feedbacks and ECS, we therefore test whether the intermodel spread in mean state high cloud characteristics relates to the intermodel spread in high cloud feedbacks. To assess differences in mean state tropical high cloud fraction among models, we compare high cloud fraction averaged from 30°N to 30°S and conditionally sampled on vertical pressure velocity at 500 hPa (ω_{500}) and pressure using output from the *cl* variable (Fig. 6a) from the piControl/piClim-control experiments. Here, the models with the highest seven ECS values (≥4.7 K) and the models with the lowest seven ECS values (≤3.7 K) are averaged into groups, and the composited conditional sampling plots are differenced. Both groups see a maximum of high cloud fraction around 200 hPa (Fig. S9), which corresponds roughly to the level of maximum detrainment (Hartmann and Larson 2002; Zelinka and Hartmann 2011). The high ECS composite demonstrates greater high cloud coverage in the upper troposphere in areas of ascent, particularly between 400 and 100 hPa. We also assess the difference in mean state tropical high cloud fraction in CTP–τ space by differencing the average piControl/piClim-control experiment cloud fraction histograms between the high and low ECS groups using output from the *clisccp* variable (Fig. 6b). While high ECS models have fewer thin high clouds than low ECS models in the 180–50 hPa bin, in sum, they exhibit greater thin high cloud fraction while low ECS models have greater thick high cloud fraction.

To understand how these mean state high cloud relationships arrange across the tropics, we visualize the spatial correlations between high cloud fraction and ECS. Thin high cloud fraction is significantly correlated with ECS in areas of strong ascent, such as the Maritime Continent, ITCZ, Amazon, West Africa, and Congo (Fig. 7a). This yields a correlation of $R = 0.50$ across areas of ascent (Fig. S10). In contrast, thick high cloud fraction is significantly anticorrelated to ECS across both areas of ascent and descent (Fig. 7b), producing a tropical mean correlation of $R = -0.60$ (Fig. S11). To consider mean high cloud opacity separate from high cloud amount, we combine thick and thin high cloud fraction by taking the ratio of thick to thin high cloud fraction and correlating it with ECS (Fig. 7c), with a higher ratio signifying thicker high clouds. The tropical mean ratio of thick to thin high cloud fraction is significantly anticorrelated to ECS, with a correlation coefficient of $R = -0.63$ (Fig. S12), albeit this relationship is influenced strongly by three MIROC models with low ECS values clustering together. This result suggests that high ECS models tend to have thinner high clouds with respect to low ECS models. Anticorrelations are strongest in areas of deep convection (Fig. 7c), but significant relationships extend across broad descent regions.

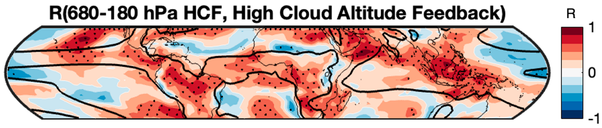

FIG. 8. Spatial correlation of 680–180 hPa cloud fraction and the total high cloud altitude feedback. The multimodel mean control experiment $\omega_{500} = 0$ hPa day^{-1} contour is depicted by the thick black line. Significance at $\alpha = 0.05$ is indicated by stippling.

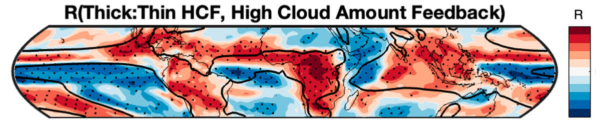

FIG. 9. Spatial correlation of ratio of mean state thick HCF to thin HCF and the total high cloud amount feedback. The multimodel mean control experiment $\omega_{500} = 0$ hPa day^{-1} contour is depicted by the thick black line. Significance at $\alpha = 0.05$ is indicated by stippling.

Having assessed the relationship between mean state high cloud characteristics and climate sensitivity, we next analyze connections between mean state high cloud fraction and the tropical high cloud feedbacks to see if climatological high clouds may mechanistically relate to ECS. First, we analyze ways in which the tropical high cloud altitude feedback is correlated with mean state variables. Ceppi et al. (2017) suggested that the high cloud altitude feedback might be related to free tropospheric cloud fraction, though this was beyond the scope of their review. To assess this hypothesis, we correlate cloud fraction between 680 and 180 hPa with the high cloud altitude feedback (Fig. 8). Because of the discretization of altitude bins using cloud fraction output from the ISCCP simulator, mean state clouds in the lowest pressure category (180–50 hPa) cannot rise to a lower pressure, so we exclude them from our quantification of mean state high cloud fraction and instead sum cloud fraction in the four pressure bins below it (680–560, 560–440, 440–310, and 310–180 hPa). Positive correlations between high cloud fraction and the altitude feedback are found in areas of deep convection such as the Amazon, equatorial Africa, and the Maritime Continent. However, these correlations are not ubiquitous across areas of ascent and are also found in subsidence regions such as the subtropical North and South Pacific basins.

Therefore, our results provide support for a relationship between mean high cloud fraction and the altitude feedback, yet this relationship is not ubiquitous throughout the tropics. Hints of this result have also been suggested in two recent studies. Findings from Po-Chedley et al. (2019) demonstrate that the rise of high clouds in GCMs can be predicted from a model's climatology, similarly suggesting that a component of the altitude feedback is related to the climatological distribution of cloud fields across altitudes. Although not explicitly computing an altitude feedback, Zelinka et al. (2022) provide additional support for this mean state relationship by showing that weather regimes dominated by high clouds see a more pronounced increase in cloud altitude under warming in comparison to regimes dominated by other cloud types. Although we find that high cloud amount correlates well with the altitude feedback in some deep convective areas, this does not fully explain the altitude feedback relationship to climate sensitivity, which we identified as being strongest across the central and eastern Pacific (Fig. 3). As a result, we suspect that other factors are acting as additional drivers of intermodel variability. Tropical upper-tropospheric warming has been shown to vary significantly across models (Mitchell et al. 2020; Keil et al. 2021), so some of the unexplained variability in our results may be related to differences in the degree of upward shifting of high clouds, as is suggested by Ceppi et al. (2017). Different representations of cloud microphysics may be playing an additional role, but analysis of this contribution is beyond the scope of this work.

As with the high cloud altitude feedback, we consider ways in which the high cloud amount and optical depth feedbacks may be related to mean state variables. We find a relationship between mean state high cloud opacity and the high cloud amount feedback, though this relationship varies between regimes of ascent and descent (Fig. 9). In areas of deep convection, the ratio of thick to thin high clouds is positively correlated with the high cloud amount feedback. We interpret this as models that simulate thicker high clouds in the mean state demonstrating a greater loss of high clouds under warming. This pattern flips outside of deep convective regions. While the strength of the correlations between the high cloud amount feedback and ECS (Fig. 5a) is weaker than the strength of the correlations between mean high cloud opacity and the high cloud amount feedback (Fig. 9), the spatial arrangement of the patterns roughly aligns. These results point to mean high cloud opacity as a potential modulator of the high cloud amount feedback wherein models with thicker high clouds in areas of climatological descent see a greater increase in high cloud amount under warming, which is modestly associated with lower climate sensitivity within our ensemble.

We speculate that different mechanisms may be driving the opposing relationships between the high cloud amount feedback and ratio of thick to thin high clouds across areas of ascent and descent. Hartmann et al. (2001) propose that a feedback process acts to maintain similar net radiation values between clear and cloudy areas in the tropics. They posit that cloud albedo and convective intensity are sensitive to changes in large-scale circulation such that a convective region with a positive radiative imbalance will experience enhanced convection and an increase in cloud opacity, thus reducing sea surface temperature (SST) gradients through a "cloud shading feedback" (Wall et al. 2019). To elaborate and place our results in the context of this purported cloud shading feedback, thin cirrus and anvils have a smaller shortwave effect than thicker high clouds (Ramanathan et al. 1989; Zelinka et al. 2012a; Hartmann and Berry 2017), allowing more incident radiation to reach the surface. Thus, alongside the expectations that tropical high clouds will decrease (Zelinka and Hartmann 2010; Bony et al. 2016) and the atmospheric overturning circulation will weaken under warming (Held and Soden 2006), the cloud shading feedback suggests that GCMs with thinner mean state high cloud fraction would experience enhanced

TABLE 1. Tropical mean correlation coefficients between high cloud feedbacks (rows) and mean state high cloud quantities (columns). Significance at $\alpha = 0.05$ is indicated by an asterisk.

	Total HCF	Thin HCF	Thick HCF	Thick:thin HCF
High cloud altitude feedback	0.53*	0.62*	0	−0.53*
High cloud optical depth feedback	0.25	0.62*	−0.45	−0.76*
High cloud amount feedback	0.68*	0.59*	0.29	−0.18

convection and a greater increase in local sea surface temperatures relative to models with a thicker cloud population through decreased stability and enhanced moisture convergence. This could mechanistically explain why thinner mean state high clouds in ascent regions are associated with a more negative high cloud amount feedback. Or, said another way, having thicker mean state high clouds would shade the surface more in a given model, muting local sea surface temperature increases and leading to a greater loss of high cloud amount in ascent regions (less detrainment from deep convection) with greenhouse gas warming compared with having thinner mean state high clouds. Wall and Hartmann (2018) argue that the cloud shading feedback could plausibly be represented by climate models given that it is constructed on mass and energy balance arguments that affect the cloud radiative effect on broad spatial scales, so we see it as applicable for understanding feedbacks within our ensemble. We additionally test the application of the cloud shading feedback to the high cloud optical depth feedback with the expectation that models with thinner high clouds in ascent regions would produce a more negative high cloud optical depth feedback (Fig. S13). However, we do not see significant correlations across tropical ascent regions as would be expected. We can also see that the cloud shading hypothesis would not apply for descent regions, as the thick to thin ratio is anticorrelated with the cloud amount feedback in these regions (Fig. 9). While we do not currently have an explanation for the descent region anticorrelation, we conjecture that the amount feedback in ascent versus descent regions is affected by different physical changes to the tropical atmosphere (e.g., convective vs microphysical).

Table 1 summarizes the tropical mean high cloud altitude, optical depth, and amount feedback correlations with mean state total high cloud fraction, thick high cloud fraction, thin high cloud fraction, and the ratio of thick to thin high cloud fraction. In general, if a model has more thin high clouds—and a greater proportion of thin high clouds—in the mean state, it will have more positive altitude and optical depth feedbacks than a model with fewer thin high clouds. This helps to explain our result shown in Fig. 6. Having more high clouds, whether thick or thin, would reasonably lead to a greater high cloud altitude feedback, yet it is unclear why a greater proportion of thin high clouds (compared to thick) would yield a more positive altitude feedback. Similarly, it is unclear exactly why a greater proportion of thin high clouds would yield a more positive optical depth feedback. Moreover, while the correlations between the amount feedback and the mean state high cloud characteristics are small in the tropical mean, recall that the local correlations can be quite large (Fig. 9), though the opposing signs of the responses in ascent vs descent regions likely explain the insignificance of the tropical mean relationships. Finally, we note that the altitude and total tropical mean state high cloud fraction (HCF) correlation, as well as the amount and total tropical mean state HCF correlation, are significantly correlated, yet the correlation is driven strongly by the two IPSL-CM6A-LR models, and thus we do not consider them to be robust.

We suspect that a nontrivial amount of the spread in mean state high cloud characteristics and the high cloud feedbacks come from the varied convective and microphysics parameterization schemes employed across the ensemble. While deep convection has a strong influence on thick high cloud fraction in areas of strong ascent, cirrus formation is also related to convection, with observations suggesting that half of tropical cirrus are formed from convective detrainment (Luo and Rossow 2004). Convective processes may influence the frequency of occurrence of thin high clouds, including both anvil cirrus and tropical tropopause layer (TTL) cirrus through mechanisms such as convective aggregation (Wing and Cronin 2016), convective detrainment (Bony et al. 2016), and entrainment of air into a convective plume (Tsushima et al. 2020) in the former and transportation of water vapor to high altitudes in the latter (Ueyama et al. 2018). Thus, it is plausible that varied convective parameterization schemes may even be responsible for high cloud characteristics and their associated changes beyond regions of strong ascent. For example, although not explicitly evaluating changes to high cloud amount in descent regions, Schiro et al. (2019) show that perturbing convective (and microphysics) parameters across a perturbed parameter ensemble (PPE) results in highly varied high cloud climatologies and responses of tropical mean high cloud fraction to interannual warming. Additionally, in their deep convection PPE, they find that the change in high cloud fraction is closely related to the magnitude of tropical ascent area fraction reduction. It then follows that variation in convective parameters across our ensemble could also create considerable spread in cloud feedbacks through their effect on changes to the tropical overturning circulation. In line with Schiro et al. (2022), we observe that low ECS models see a greater weakening of the atmospheric overturning circulation than high ECS models in the perturbed scenario (Fig. S14), which they associate with a smaller decrease in tropical ascent area and lesser decrease in tropical high cloud fraction with warming. To what extent changes to the tropical overturning circulation relate to diversity in deep convective characteristics across ensemble members and how this relates to high cloud feedbacks is, however, beyond the scope of this study.

In addition to the representation of deep convection, recent work has highlighted microphysical parameters and processes such as ice autoconversion size threshold (Duffy et al. 2024), cloud lifetime and decay (Seeley et al. 2019), and ice fall speed and density (Schiro et al. 2019; Tsushima et al. 2020; Wang et al. 2020) as factors impacting anvil cloud fraction. Additionally, intermodel comparisons of global storm-resolving models—which explicitly simulate convection but parameterize cloud microphysics—find significantly variable cloud radiative effects of tropical cirrus across microphysics schemes (Turbeville et al. 2022; Atlas et al. 2024). Thus, we suspect that microphysics parameterization diversity is a large driver of intermodel spread in mean state high cloud characteristics and high cloud feedbacks, particularly in regions of large-scale descent. However, because it is difficult to differentiate the effects of microphysical and deep convective parameterizations in an intermodel comparison, we are limited to speculation in the absence of a comprehensive PPE ensemble and analysis aimed at addressing these questions.

4. Conclusions

In this work, we conclude that the intermodel variability of the tropical high cloud altitude and optical depth feedbacks is related to the spread of equilibrium climate sensitivity at the tropics-wide scale. Assessing the spatial correlations of the tropical net high cloud feedback to ECS illustrates that the strongest relationships exist outside of regions of deepest climatological ascent, reflective of the relationship between ECS and the diverse responses of anvils and thin cirrus extending away from deep convective zones. The intermodel variability of high cloud feedbacks in regions where optically thin high clouds dominate has not been emphasized in the literature, aside from recent work by Sokol et al. (2024) looking across an ensemble of idealized convection permitting simulations, but given the difficulty with which coarse models represent cirrus (Sherwood et al. 2020; Gasparini et al. 2023) and the multitude of factors previously highlighted that impact cirrus amount and radiative properties in GCMs, our result is somewhat unsurprising.

We also assess the extent to which the intermodel variability of climatological high cloud characteristics is related to the spread of the high cloud feedbacks and ECS. As the feedbacks can be decomposed into the product of the mean state high cloud properties, change in high cloud properties, and changes in radiative properties, we wonder to what extent the mean state high cloud properties dominate the intermodel spread in the feedbacks. We find that greater mean state high cloud fraction is present in higher ECS models, though the clouds are thinner: higher ECS models simulate greater thin high cloud coverage across tropical ascent regions and fewer thick high clouds broadly across the tropics. Finally, we highlight significant positive correlations between thin, mean-state, tropical mean high cloud amount and both the tropical mean high cloud altitude and optical depth feedbacks. Greater mean state cloudiness of any optical thickness would be expected to amplify the altitude feedback, but it is less obvious why greater thin high cloud fraction should amplify the optical depth feedback. While we only consider correlations between high cloud feedbacks and ECS, analysis of how high cloud opacity could be linked to other changes in the atmosphere that influence other feedback components that vary strongly with ECS could be a direction for future work. Finally, no significant relationship exists between the mean state high cloud amount and the high cloud amount feedback in the tropical mean, yet we see significant positive local correlations in ascent regions and significant negative local correlations in descent regions. We hypothesize that a cloud shading mechanism may be acting within ascent regions to drive these positive correlations between the mean state cloud amount and the amount feedback, whereas changes to cloud microphysics may be driving the relationship to be of opposite sign in the descent regions.

Given the significant, positive correlations between the tropical high cloud altitude and optical depth feedbacks and ECS, in addition to the significant relationships between mean state high cloud characteristics and these feedbacks across our ensemble, we underscore these results as an opportunity to consider an emergent constraint. Disentangling the underlying drivers of these correlations, whether that be cloud microphysics schemes, deep convective parameterizations, additional mean state parameters, or variability in the response of other components of the modeled atmosphere to warming, remains an important task. Solidifying a mechanistic understanding of the mean state relationships to the high cloud feedbacks and climate sensitivity is a crucial step toward creating a new emergent constraint. Moreover, while spread in modeled high cloud climatology could be contributing nontrivially and systematically to the spread in high cloud feedbacks, as we presented here, additional factors that we did not explore in this study are also likely contributors. These factors may include intermodel variability in responses of precipitation efficiency, the overturning circulation, convective organization, tropical tropospheric stability, and/or the height of maximum detrainment to surface warming, which may themselves provide opportunities for constraining high cloud feedbacks.

Finally, we acknowledge the possibility that high cloud feedbacks could be related to low cloud feedbacks, as high and low cloud changes are likely to be coupled through changes in tropospheric stability and the tropical overturning circulation (Schiro et al. 2022). Thus, we also acknowledge the nonzero likelihood that certain correlations with ECS presented here are influenced nontrivially by high cloud feedback relationships to other cloud changes or atmospheric processes that drive substantial spread in ECS. Nevertheless, we stress the need to strongly consider tropical high cloud contributions, particularly the high cloud altitude and optical depth feedbacks, to the intermodel spread in ECS in efforts to constrain future warming.

Acknowledgments. The authors acknowledge funding support from the National Science Foundation (Grant 2225954), the Department of Energy's Regional and Global Modeling and Analysis (DOE RGMA) program, and the University of Virginia. The authors thank Mark Zelinka for feedback and many useful discussions throughout the writing process and three anonymous reviewers for their constructive reviews and helpful feedback, which significantly improved the manuscript.

Data availability statement. Output from the CMIP5 and CMIP6 models used in this study can be found on the Earth System Grid Federation (ESGF; https://aims2.llnl.gov/search/cmip6/) through the Program for Climate Model Diagnosis and Intercomparison (PCMDI) at Lawrence Livermore National Laboratory. Analysis scripts can be found at https://schiro.evsc.virginia.edu/index.php/data/.

REFERENCES

Atlas, R. L., C. S. Bretherton, A. B. Sokol, P. N. Blossey, and M. F. Khairoutdinov, 2024: Tropical cirrus are highly sensitive to ice microphysics within a nudged global storm-resolving model. *Geophys. Res. Lett.*, **51**, e2023GL105868, https://doi.org/10.1029/2023GL105868.

Beydoun, H., P. M. Caldwell, W. M. Hannah, and A. S. Donahue, 2021: Dissecting anvil cloud response to sea surface warming. *Geophys. Res. Lett.*, **48**, e2021GL094049, https://doi.org/10.1029/2021GL094049.

Bony, S., and J.-L. Dufresne, 2005: Marine boundary layer clouds at the heart of tropical cloud feedback uncertainties in climate models. *Geophys. Res. Lett.*, **32**, L20806, https://doi.org/10.1029/2005GL023851.

——, B. Stevens, D. Coppin, T. Becker, K. A. Reed, A. Voigt, and B. Medeiros, 2016: Thermodynamic control of anvil cloud amount. *Proc. Natl. Acad. Sci. USA*, **113**, 8927–8932, https://doi.org/10.1073/pnas.1601472113.

Brient, F., and T. Schneider, 2016: Constraints on climate sensitivity from space-based measurements of low-cloud reflection. *J. Climate*, **29**, 5821–5835, https://doi.org/10.1175/JCLI-D-15-0897.1.

——, ——, Z. Tan, S. Bony, X. Qu, and A. Hall, 2016: Shallowness of tropical low clouds as a predictor of climate models' response to warming. *Climate Dyn.*, **47**, 433–449, https://doi.org/10.1007/s00382-015-2846-0.

Caldwell, P. M., M. D. Zelinka, K. E. Taylor, and K. Marvel, 2016: Quantifying the sources of intermodel spread in equilibrium climate sensitivity. *J. Climate*, **29**, 513–524, https://doi.org/10.1175/JCLI-D-15-0352.1.

Ceppi, P., F. Brient, M. D. Zelinka, and D. L. Hartmann, 2017: Cloud feedback mechanisms and their representation in global climate models. *Wiley Interdiscip. Rev.: Climate Change*, **8**, e465, https://doi.org/10.1002/wcc.465.

Chao, L.-W., M. D. Zelinka, and A. E. Dessler, 2024: Evaluating cloud feedback components in observations and their representation in climate models. *J. Geophys. Res. Atmos.*, **129**, e2023JD039427, https://doi.org/10.1029/2023JD039427.

Choi, Y.-S., W. Kim, S.-W. Yeh, H. Masunaga, M.-J. Kwon, H.-S. Jo, and L. Huang, 2017: Revisiting the iris effect of tropical cirrus clouds with TRMM and a-train satellite data. *J. Geophys. Res. Atmos.*, **122**, 5917–5931, https://doi.org/10.1002/2016JD025827.

Cronin, T. W., and A. A. Wing, 2017: Clouds, circulation, and climate sensitivity in a radiative-convective equilibrium channel model. *J. Adv. Model. Earth Syst.*, **9**, 2883–2905, https://doi.org/10.1002/2017MS001111.

Duffy, M. L., B. Medeiros, A. Gettelman, and T. Eidhammer, 2024: Perturbing parameters to understand cloud contributions to climate change. *J. Climate*, **37**, 213–227, https://doi.org/10.1175/JCLI-D-23-0250.1.

Dufresne, J.-L., and S. Bony, 2008: An assessment of the primary sources of spread of global warming estimates from coupled atmosphere–ocean models. *J. Climate*, **21**, 5135–5144, https://doi.org/10.1175/2008JCLI2239.1.

Gasparini, B., P. J. Rasch, D. L. Hartmann, C. J. Wall, and M. Dütsch, 2021: A Lagrangian perspective on tropical anvil cloud lifecycle in present and future climate. *J. Geophys. Res. Atmos.*, **126**, e2020JD033487, https://doi.org/10.1029/2020JD033487.

——, S. C. Sullivan, A. B. Sokol, B. Kärcher, E. Jensen, and D. L. Hartmann, 2023: Opinion: Tropical cirrus—From micro-scale processes to climate-scale impacts. *Atmos. Chem. Phys.*, **23**, 15 413–15 444, https://doi.org/10.5194/acp-23-15413-2023.

Gregory, J. M., and Coauthors, 2004: A new method for diagnosing radiative forcing and climate sensitivity. *Geophys. Res. Lett.*, **31**, L03205, https://doi.org/10.1029/2003GL018747.

Hartmann, D. L., 2016: Tropical anvil clouds and climate sensitivity. *Proc. Natl. Acad. Sci. USA*, **113**, 8897–8899, https://doi.org/10.1073/pnas.1610455113.

——, and K. Larson, 2002: An important constraint on tropical cloud—climate feedback. *Geophys. Res. Lett.*, **29**, 1951, https://doi.org/10.1029/2002GL015835.

——, and S. E. Berry, 2017: The balanced radiative effect of tropical anvil clouds. *J. Geophys. Res. Atmos.*, **122**, 5003–5020, https://doi.org/10.1002/2017JD026460.

——, L. A. Moy, and Q. Fu, 2001: Tropical convection and the energy balance at the top of the atmosphere. *J. Climate*, **14**, 4495–4511, https://doi.org/10.1175/1520-0442(2001)014<4495:TCATEB>2.0.CO;2.

Held, I. M., and B. J. Soden, 2006: Robust responses of the hydrological cycle to global warming. *J. Climate*, **19**, 5686–5699, https://doi.org/10.1175/JCLI3990.1.

Houze, R. A., Jr., K. L. Rasmussen, M. D. Zuluaga, and S. R. Brodzik, 2015: The variable nature of convection in the tropics and subtropics: A legacy of 16 years of the tropical rainfall measuring mission satellite. *Rev. Geophys.*, **53**, 994–1021, https://doi.org/10.1002/2015RG000488.

Jeevanjee, N., and L. Zhou, 2022: On the resolution-dependence of anvil cloud fraction and precipitation efficiency in radiative-convective equilibrium. *J. Adv. Model. Earth Syst.*, **14**, e2021MS002759, https://doi.org/10.1029/2021MS002759.

Keil, P., H. Schmidt, B. Stevens, and J. Bao, 2021: Variations of tropical lapse rates in climate models and their implications for upper-tropospheric warming. *J. Climate*, **34**, 9747–9761, https://doi.org/10.1175/JCLI-D-21-0196.1.

Klein, S. A., and C. Jakob, 1999: Validation and sensitivities of frontal clouds simulated by the ECMWF model. *Mon. Wea. Rev.*, **127**, 2514–2531, https://doi.org/10.1175/1520-0493(1999)127<2514:VASOFC>2.0.CO;2.

——, and A. Hall, 2015: Emergent constraints for cloud feedbacks. *Curr. Climate Change Rep.*, **1**, 276–287, https://doi.org/10.1007/s40641-015-0027-1.

Lindzen, R. S., M.-D. Chou, and A. Y. Hou, 2001: Does the earth have an adaptive infrared iris? *Bull. Amer. Meteor. Soc.*, **82**, 417–432, https://doi.org/10.1175/1520-0477(2001)082<0417:DTEHAA>2.3.CO;2.

Liu, R., K.-N. Liou, H. Su, Y. Gu, B. Zhao, J. H. Jiang, and S. C. Liu, 2017: High cloud variations with surface temperature from 2002 to 2015: Contributions to atmospheric radiative cooling rate and precipitation changes. *J. Geophys. Res. Atmos.*, **122**, 5457–5471, https://doi.org/10.1002/2016JD026303.

Luo, Z., and W. B. Rossow, 2004: Characterizing tropical cirrus life cycle, evolution, and interaction with upper-tropospheric water vapor using Lagrangian trajectory analysis of satellite observations. *J. Climate*, **17**, 4541–4563, https://doi.org/10.1175/3222.1.

McKim, B., S. Bony, and J.-L. Dufresne, 2024: Weak anvil cloud area feedback suggested by physical and observational constraints. *Nat. Geosci.*, **17**, 392–397, https://doi.org/10.1038/s41561-024-01414-4.

Mitchell, D. M., Y. T. Eunice Lo, W. J. M. Seviour, L. Haimberger, and L. M. Polvani, 2020: The vertical profile of recent tropical temperature trends: Persistent model biases in the context of internal variability. *Environ. Res. Lett.*, **15**, 1040b4, https://doi.org/10.1088/1748-9326/ab9af7.

Ohno, T., M. Satoh, and A. Noda, 2019: Fine vertical resolution radiative-convective equilibrium experiments: Roles of turbulent mixing on the high-cloud response to sea surface temperatures. *J. Adv. Model. Earth Syst.*, **11**, 1637–1654, https://doi.org/10.1029/2019MS001704.

Pincus, R., S. Platnick, S. A. Ackerman, R. S. Hemler, and R. J. P. Hofmann, 2012: Reconciling simulated and observed views of clouds: MODIS, ISCCP, and the limits of instrument simulators. *J. Climate*, **25**, 4699–4720, https://doi.org/10.1175/JCLI-D-11-00267.1.

Po-Chedley, S., M. D. Zelinka, N. Jeevanjee, T. J. Thorsen, and B. D. Santer, 2019: Climatology explains intermodel spread in tropical upper tropospheric cloud and relative humidity response to greenhouse warming. *Geophys. Res. Lett.*, **46**, 13 399–13 409, https://doi.org/10.1029/2019GL084786.

Raghuraman, S. P., B. Medeiros, and A. Gettelman, 2024: Observational quantification of tropical high cloud changes and feedbacks. *J. Geophys. Res. Atmos.*, **129**, e2023JD039364, https://doi.org/10.1029/2023JD039364.

Ramanathan, V., R. D. Cess, E. F. Harrison, P. Minnis, B. R. Barkstrom, E. Ahmad, and D. Hartmann, 1989: Cloud-radiative forcing and climate: Results from the Earth radiation budget experiment. *Science*, **243**, 57–63, https://doi.org/10.1126/science.243.4887.57.

Richardson, M. T., R. J. Roy, and M. D. Lebsock, 2022: Satellites suggest rising tropical high cloud altitude: 2002–2021. *Geophys. Res. Lett.*, **49**, e2022GL098160, https://doi.org/10.1029/2022GL098160.

Saint-Lu, M., S. Bony, and J.-L. Dufresne, 2020: Observational evidence for a stability Iris effect in the tropics. *Geophys. Res. Lett.*, **47**, e2020GL089059, https://doi.org/10.1029/2020GL089059.

Sassen, K., Z. Wang, and D. Liu, 2009: Cirrus clouds and deep convection in the tropics: Insights from CALIPSO and CloudSat. *J. Geophys. Res.*, **114**, D001106, https://doi.org/10.1029/2009JD011916.

Schiro, K. A., H. Su, Y. Wang, B. Langenbrunner, J. H. Jiang, and J. D. Neelin, 2019: Relationships between tropical ascent and high cloud fraction changes with warming revealed by perturbation physics experiments in CAM5. *Geophys. Res. Lett.*, **46**, 10 112–10 121, https://doi.org/10.1029/2019GL083026.

——, and Coauthors, 2022: Model spread in tropical low cloud feedback tied to overturning circulation response to warming. *Nat. Commun.*, **13**, 7119, https://doi.org/10.1038/s41467-022-34787-4.

Seeley, J. T., N. Jeevanjee, W. Langhans, and D. M. Romps, 2019: Formation of tropical anvil clouds by slow evaporation. *Geophys. Res. Lett.*, **46**, 492–501, https://doi.org/10.1029/2018GL080747.

Sherwood, S. C., and Coauthors, 2020: An assessment of Earth's climate sensitivity using multiple lines of evidence. *Rev. Geophys.*, **58**, e2019RG000678, https://doi.org/10.1029/2019RG000678.

Siler, N., S. Po-Chedley, and C. S. Bretherton, 2018: Variability in modeled cloud feedback tied to differences in the climatological spatial pattern of clouds. *Climate Dyn.*, **50**, 1209–1220, https://doi.org/10.1007/s00382-017-3673-2.

Soden, B. J., and I. M. Held, 2006: An assessment of climate feedbacks in coupled ocean–atmosphere models. *J. Climate*, **19**, 3354–3360, https://doi.org/10.1175/JCLI3799.1.

Sokol, A. B., C. J. Wall, and D. L. Hartmann, 2024: Greater climate sensitivity implied by anvil cloud thinning. *Nat. Geosci.*, **17**, 398–403, https://doi.org/10.1038/s41561-024-01420-6.

Su, H., J. H. Jiang, C. Zhai, T. J. Shen, J. D. Neelin, G. L. Stephens, and Y. L. Yung, 2014: Weakening and strengthening structures in the Hadley Circulation change under global warming and implications for cloud response and climate sensitivity. *J. Geophys. Res. Atmos.*, **119**, 5787–5805, https://doi.org/10.1002/2014JD021642.

——, and Coauthors, 2017: Tightening of tropical ascent and high clouds key to precipitation change in a warmer climate. *Nat. Commun.*, **8**, 15771, https://doi.org/10.1038/ncomms15771.

Tsushima, Y., M. A. Ringer, G. M. Martin, J. W. Rostron, and D. M. H. Sexton, 2020: Investigating physical constraints on climate feedbacks using a perturbed parameter ensemble. *Climate Dyn.*, **55**, 1159–1185, https://doi.org/10.1007/s00382-020-05318-y.

Turbeville, S. M., J. M. Nugent, T. P. Ackerman, C. S. Bretherton, and P. N. Blossey, 2022: Tropical cirrus in global storm-resolving models: 2. Cirrus life cycle and top-of-atmosphere radiative fluxes. *Earth Space Sci.*, **9**, e2021EA001978, https://doi.org/10.1029/2021EA001978.

Ueyama, R., E. J. Jensen, and L. Pfister, 2018: Convective influence on the humidity and clouds in the tropical tropopause layer during boreal summer. *J. Geophys. Res. Atmos.*, **123**, 7576–7593, https://doi.org/10.1029/2018JD028674.

Vial, J., J.-L. Dufresne, and S. Bony, 2013: On the interpretation of inter-model spread in CMIP5 climate sensitivity estimates. *Climate Dyn.*, **41**, 3339–3362, https://doi.org/10.1007/s00382-013-1725-9.

Volodin, E. M., 2008: Relation between temperature sensitivity to doubled carbon dioxide and the distribution of clouds in current climate models. *Izv., Atmos. Ocean. Phys.*, **44**, 288–299, https://doi.org/10.1134/S0001433808030043.

Wall, C. J., and D. L. Hartmann, 2018: Balanced cloud radiative effects across a range of dynamical conditions over the tropical west Pacific. *Geophys. Res. Lett.*, **45**, 11 490–11 498, https://doi.org/10.1029/2018GL080046.

——, ——, and J. R. Norris, 2019: Is the net cloud radiative effect constrained to be uniform over the tropical warm pools? *Geophys. Res. Lett.*, **46**, 12 495–12 503, https://doi.org/10.1029/2019GL083642.

Wang, Y., H. Su, J. H. Jiang, F. Xu, and Y. L. Yung, 2020: Impact of cloud ice particle size uncertainty in a climate model and implications for future satellite missions. *J. Geophys. Res. Atmos.*, **125**, e2019JD032119, https://doi.org/10.1029/2019JD032119.

Wing, A. A., and T. W. Cronin, 2016: Self-aggregation of convection in long channel geometry. *Quart. J. Roy. Meteor. Soc.*, **142** (694), 1–15, https://doi.org/10.1002/qj.2628.

——, and Coauthors, 2020: Clouds and convective self-aggregation in a multimodel ensemble of radiative-convective equilibrium simulations. *J. Adv. Model. Earth Syst.*, **12**, e2020MS002138, https://doi.org/10.1029/2020MS002138.

Xu, K.-M., T. Wong, B. A. Wielicki, L. Parker, B. Lin, Z. A. Eitzen, and M. Branson, 2007: Statistical analyses of satellite cloud object data from CERES. Part II: Tropical convective cloud objects during 1998 El Niño and evidence for supporting the fixed anvil temperature hypothesis. *J. Climate*, **20**, 819–842, https://doi.org/10.1175/JCLI4069.1.

Zelinka, M. D., and D. L. Hartmann, 2010: Why is longwave cloud feedback positive? *J. Geophys. Res.*, **115**, D16117, https://doi.org/10.1029/2010JD013817.

——, and ——, 2011: The observed sensitivity of high clouds to mean surface temperature anomalies in the tropics. *J. Geophys. Res.*, **116**, D23103, https://doi.org/10.1029/2011JD016459.

——, S. A. Klein, and D. L. Hartmann, 2012a: Computing and partitioning cloud feedbacks using cloud property histograms. Part I: Cloud radiative kernels. *J. Climate*, **25**, 3715–3735, https://doi.org/10.1175/JCLI-D-11-00248.1.

——, ——, and ——, 2012b: Computing and partitioning cloud feedbacks using cloud property histograms. Part II: Attribution to changes in cloud amount, altitude, and optical depth. *J. Climate*, **25**, 3736–3754, https://doi.org/10.1175/JCLI-D-11-00249.1.

——, ——, K. E. Taylor, T. Andrews, M. J. Webb, J. M. Gregory, and P. M. Forster, 2013: Contributions of different cloud types to feedbacks and rapid adjustments in CMIP5. *J. Climate*, **26**, 5007–5027, https://doi.org/10.1175/JCLI-D-12-00555.1.

——, C. Zhou, and S. A. Klein, 2016: Insights from a refined decomposition of cloud feedbacks. *Geophys. Res. Lett.*, **43**, 9259–9269, https://doi.org/10.1002/2016GL069917.

——, T. A. Myers, D. T. McCoy, S. Po-Chedley, P. M. Caldwell, P. Ceppi, S. A. Klein, and K. E. Taylor, 2020: Causes of higher climate sensitivity in CMIP6 models. *Geophys. Res. Lett.*, **47**, e2019GL085782, https://doi.org/10.1029/2019GL085782.

——, S. A. Klein, Y. Qin, and T. A. Myers, 2022: Evaluating climate models' cloud feedbacks against expert judgment. *J. Geophys. Res. Atmos.*, **127**, e2021JD035198, https://doi.org/10.1029/2021JD035198.

Zhai, C., J. H. Jiang, and H. Su, 2015: Long-term cloud change imprinted in seasonal cloud variation: More evidence of high climate sensitivity. *Geophys. Res. Lett.*, **42**, 8729–8737, https://doi.org/10.1002/2015GL065911.

Zhou, C., A. E. Dessler, M. D. Zelinka, P. Yang, and T. Wang, 2014: Cirrus feedback on interannual climate fluctuations. *Geophys. Res. Lett.*, **41**, 9166–9173, https://doi.org/10.1002/2014GL062095.